Evidence for multi-gap symmetry from grain boundary effects in polycrystalline $Ba_{0.6}K_{0.4}Fe_2As_2$ microbridge

You may also be interested in:

Evidence for multi-gap symmetry from grain boundary effects in polycrystalline Ba$_{0.6}$K$_{0.4}$Fe$_2$As$_2$ microbridge

Ya Huang[1,2]**, Xian-Jing Zhou**[1,2]**, Zhao-Shun Gao**[2,3]**, Hao Wu**[2,4]**, Ge He**[5]**,
Jie Yuan**[5]**, Kui Jin**[5]**, Paulo J Pereira**[6,7]**, Min Ji**[1,2]**, De-Yue An**[1,2]**, Jun Li**[1,8]**,
Takeshi Hatano**[2]**, Biao-Bing Jin**[1]**, Hua-Bing Wang**[1,2,8] **and Pei-Heng Wu**[1]

[1] Research Institute of Superconductor Electronics, Nanjing University, Nanjing 210093, People's Republic of China
[2] National Institute for Materials Science, Tsukuba 3050047, Japan
[3] Institute of Electrical Engineering, Chinese Academy of Sciences, Beijing 100190, People's Republic of China
[4] Wuhan University, Wuhan 430047, People's Republic of China
[5] Condensed Matter Physics, Institute of Physics, Chinese Acadamy of Sciences, Beijing 100190, People's Republic of China
[6] INPAC-Institute for Nanoscale Physics and Chemistry, KU Leuven, Celestijnenlaan 200 D, Leuven B-3001, Belgium
[7] Theory of Nanomaterials Group, KU Leuven, Leuven B-3001, Belgium

E-mail: junli@nju.edu.cn and hbwang1000@gmail.com

Abstract
We studied the grain boundaries within mechanically formed polycrystalline Ba$_{0.6}$K$_{0.4}$Fe$_2$As$_2$ micro-bridges. By tunneling current across grain boundaries, current–voltage characteristics (IVCs) demonstrated the typical Josephson weak links behavior in micro-bridges. Shapiro steps were observed for the junctions under the microwave radiation at 10 GHz. The temperature dependence of the critical current I_c was observed as a shoulder, corresponding to a multi-gap symmetry but not a single-gap s-wave or d-wave.

Keywords: grain boundary effect, Josephson junction, multi-gap symmetry, iron-based superconductors

(Some figures may appear in colour only in the online journal)

1. Introduction

The superconducting (SC) mechanism for the newly discovered Fe-based superconductors (FeSCs) is still an open question [1, 2] in regards to high critical temperature (T_c) cuprate superconductors. To elucidate the pairing mechanism, it is crucial to probe the symmetry of the SC phase and then present the Cooper pairing dependent energy and momentum [2]. Theoretical scientists have proposed several possible models, including the single-gap s- and d-state, and the multi-gap $s_{\pm}$ [3, 4], s_{++} wave [5–7], and $s + \mathrm{i}d$-wave [8]. Singlet symmetry,

such as the s- and d-state, was determined by NMR experiments from Knight shift measurements [9–11] in several systems including the 1111-, 122- and 11-systems. However, the multi-gap s-wave ($s_{\pm}$ or s_{++}) is generally accepted. Both states represent the same hole Fermi pockets, and have opposite signs for the electron pockets; namely, the $s_{\pm}$ wave is a sign-reversal s-wave model, and a non-sign-reversal for the s_{++} state. Multi-gap symmetry was supported by Josephson tunneling [12, 13], angle-resolved photoemission spectroscopy (ARPES) [14], London penetration [15], and impurity doping [16] experiments. Among these methods, the Josephson tunneling effect is powerful owing to phase- and amplitude-sensitivity, making it possible to distinguish the multi-gap from the single-gap.

[8] Authors to whom any correspondence should be addressed.

Until now, few Josephson effect experiments on FeSCs have been reported. Zhang et al [12] fabricated a hysteretic junction between Pb and $(Ba,K)Fe_2As_2$. The observation of robust Josephson coupling and current–voltage characteristics (IVCs) suggested the exclusion of predominant p-wave symmetry, but can hardly identify the multi-gap s-wave from the d-wave. Integer and half-integer flux quantum in polycrystalline $NdFeAsO_{0.88}F_{0.12}$ [13] also supported s± or d-wave pairing, but ruled out p-wave pairing. On the other hand, a thin-film bicrystal technique with grain boundary was widely used to study the Josephson tunneling effect. Bicrystals can be easily fabricated and therefore have been applied in various SC devices for several decades, including cuprates- [17, 18] and MgB_2-based [19] superconductors. Although Fe-based thin films have been fabricated successfully in several systems, including Fe(Se,Te) [20], $Ba(Fe,Co)_2As_2$ [21–23], and $LaFeAsO_{1-x}F_x$ [24], there are still some technical difficulties for bicrystal study in FeSCs. Alternatively, polycrystals is another promising way to study the grain boundary because a great number of single crystalline grains connect each other to natural grain boundaries [13].

In the present work, we will discuss the IVCs and temperature dependence of the critical current I_c for grain boundary junctions in polycrystalline $Ba_{0.6}K_{0.4}Fe_2As_2$ microbridges. Microwave radiation at 10 GHz was applied to the junctions to confirm Josephson coupling. In particular, the I_c–T relation was studied to understand the influence of the order parameter symmetry on the behavior of the Josephson tunneling junction. The experimental data also will also be compared with the theoretical prediction for the simple s- and d-wave, and the multi-gap s-wave.

2. Experimental methods

The synthesis of $Ba_{0.6}K_{0.4}Fe_2As_2$ polycrystals was described elsewhere [25]. Previous microscopic analysis demonstrated a denser and uniform micro-structure for the $Ba_{0.6}K_{0.4}Fe_2As_2$ polycrystals due to the rolling process under high pressure. Figure 1(b) shows a scanning electron microscopic image for the enlarged view of the polyscrystal. The fine single crystalline grains were randomly oriented within the bulk crystal and connected to each other with a misoriented angle, resulting in abundant grain boundaries. Grains were observed having a width of 1–5 μm. We selected a bulk polycrystal and polished it to a thickness of 100–200 μm, and then mounted it onto a MgO substrate using epoxy (EPO-TEK, 353ND04), and heat-treated it at 110 °C for 2–3 h. Finally, the thin region was then cut into a microbridge using a sharp knife, as shown in the inset of figure 1(a). Figure 1(a) shows the schematic view of the microbridge and electrodes. We emphasize that the cross-sectional area of the microbridge was gradually shrunk until the two-terminal resistance reached a few ohm. The microbridge was connected to Au wires using silver paste for electrodes. The transport properties of the junctions were measured in a Janis helium flow cryostat.
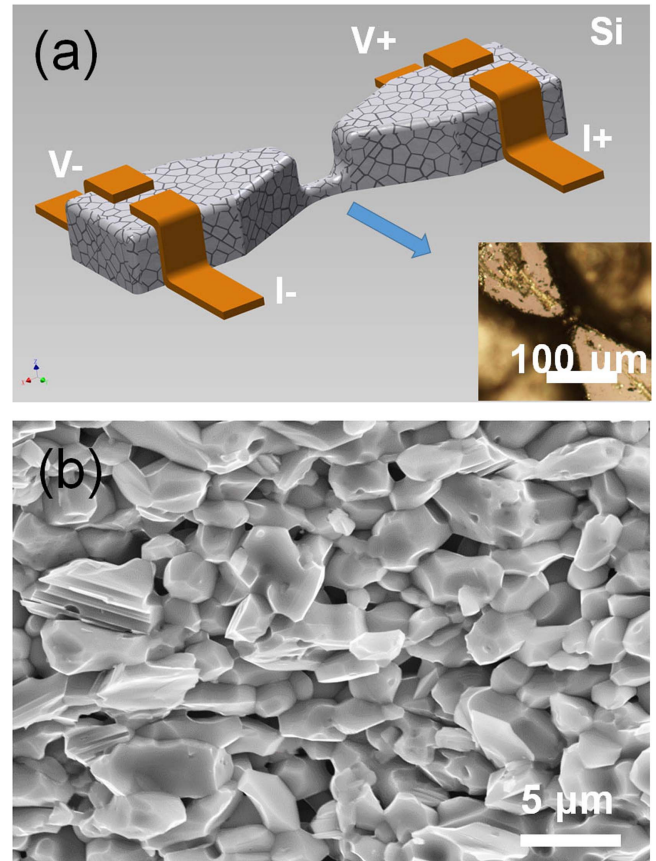
Figure 1. (a) Schematic image of junctions with width of 20 μm. Inset shows optical image for the enlarged view of the microbridge. (b) Scanning electron microscopic image for the polycrystal.

3. Results and discussion

The temperature dependence of resistance R for a microbridge is given in figure 2. The onset T_c is about 35.1 K, being similar in behavior as that of the bulk crystal [25]. Since the microbridge cross-section is considerably less than that of the electrodes, the total resistance can be attributed to the microbridge. According to our previous measurements on $Ba_{0.6}K_{0.4}Fe_2As_2$ polycrystals [25], the normal state resistivity at 38 K is around 100 $\mu\Omega \cdot$ cm. Thus, we can roughly estimate the cross-sectional area of the microbridge as 28.6 μm^2.

Figure 3 shows the IVCs of the microbridge with or without microwave irradiation at 10 GHz. The power ranges from 7 to 23 dBm. Without microwave irradiation, the IVC was recorded by sweeping the current up and down through the microbridge from −30 to 30 mA. The critical current density J_c was estimated as 62.9 kA cm^{-2} for the microbridge at 10 K, which was considerably less than the Ginzburg–Landau limit of supercurrent capacities for $Ba_{0.6}K_{0.4}Fe_2As_2$ superconductors, regardless of the ab-plane or c-axis. The ab-plane depairing current density of the $Ba_{0.5}K_{0.5}Fe_2As_2$ patterned microbridge was as high as 10.8 MA cm^{-2} at 4 K [26]. Additionally, the present $Ba_{0.6}K_{0.4}Fe_2As_2$ microbridge demonstrated no obvious flux-flow behavior from $R − T$ and IVC curves. Furthermore, the flux motion dominated J_c was in a magnitude of MA/cm^2 in a
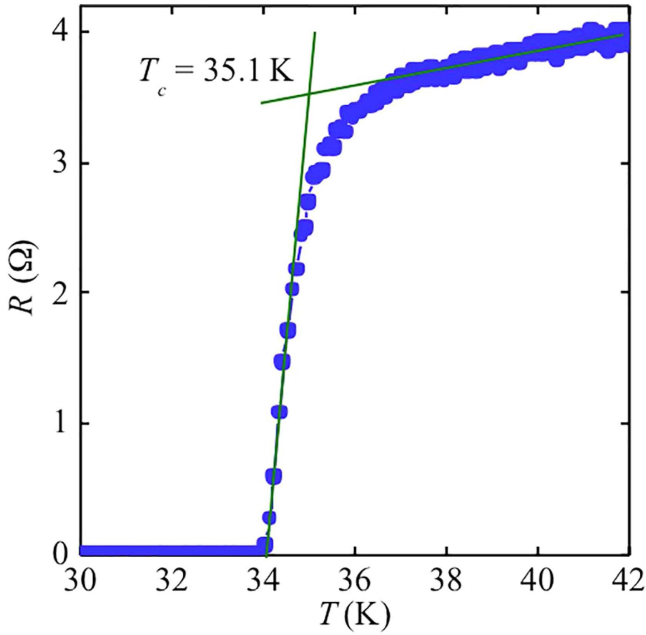
Figure 2. Temperature dependence of resistance *R*. The determination procedure of T_c is indicated as oliver lines.
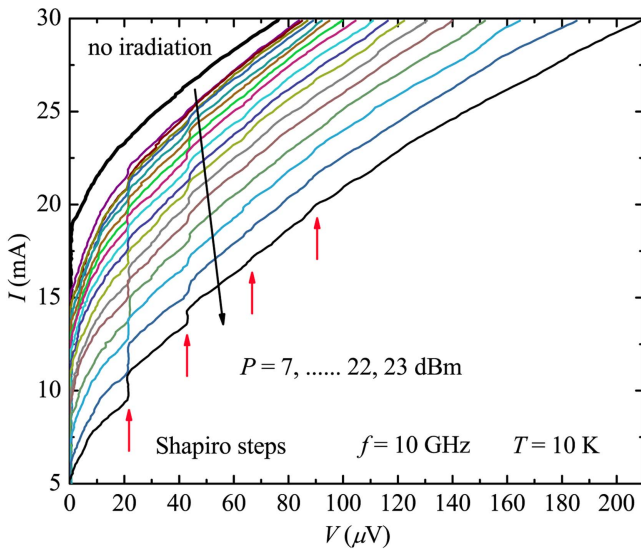
Figure 3. IVCs of the microbridge in the presence of a microwave current of frequency 10 GHz and powers from 7 dBm to 23 dBm. Blue arrows index the Shapiro steps. Bath temperature was fixed at 10 K and microwave was introduced by direct conductive coupling to the sample.

pure crystal [27], about two orders of magnitude higher than the present J_c. Therefore, we ascribe the considerably less J_c to the grain boundaries rather than to flux motion or depairing.

When the current was reduced, the curve returned to the resistive branch without hysteresis, indicating a resistively shunted junction [17, 28]. The profile of the present IVCs resembles that of the YBa$_2$Cu$_3$O$_{7-x}$(YBCO) grain boundary junctions, but with remarkable excess current. At 10 K, $I_c R_n$ of the whole microbridge is about 70 mV (R_n is the normal resistance), much larger than the value estimated at the
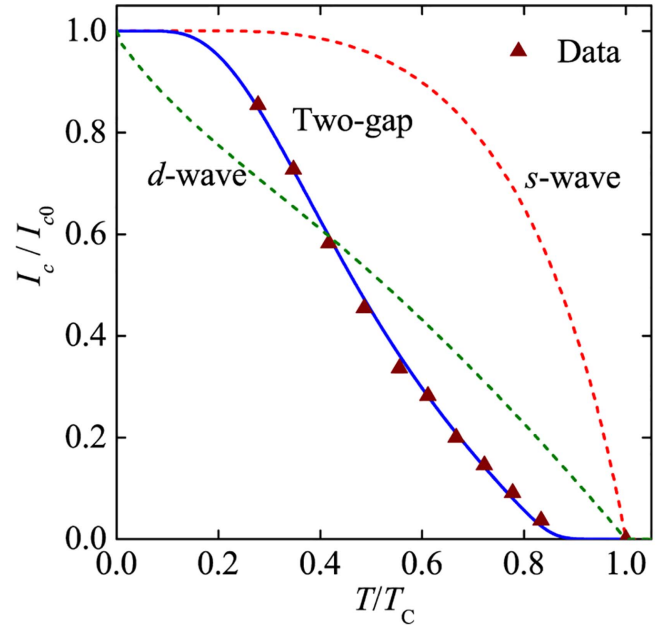
Figure 4. Normalized temperature (T/T_c) dependence of the normalized I_c/I_{c0}. The triangle dots display the experimental data. The red, green, and blue lines represent the calculated data from the Ambegaokar–Baratoff relation for the *s*-wave, *d*-wave, and two-gap models, respectively.

superconducting gap (as an order of micro-voltage for the 122-type [28]), suggesting that a great number of grain boundary junctions exist in series in this microbridge. Although we cannot confirm the grain boundary geometry from the scanning electron microscopic image, grain connections should be intense due to the extremely low coherence length of the high-T_c Fe-based superconductors, which is normally below 2 nm at temperatures far below the T_C [26].

When the junctions were irradiated with microwaves at 10 GHz, the IVCs demonstrated a series of pronounced Shaprio steps. The Shaprio steps were observed with voltage interval ΔV of around 21 μV. The interval voltage ΔV satisfied Josephson relation

$$\Delta V = f \cdot \Phi_0, \qquad (1)$$

where f is the microwave frequency and Φ_0 is the flux quantum [17].

To investigate the influence of the order parameters on the behavior of the Josephson junction, it is essential to know the temperature dependence of the critical current. In figure 4, the experimental data of the normalized I_c/I_{c0} is plotted as function of normalized temperature T/T_c, where, I_{c0} is the critical current at 0 K. To study $(I_c/I_{c0}) - (T/T_c)$ curves within various gap symmetry models, we applied the single-gap model of the *s*-wave and *d*-wave and an effective two-gap superconductor model, similar to those in MgB$_2$ calculations. To simplify beginning calculations, we considered the weak coupling regime for order parameter calculations in the two-gap model. We used the standard self-consistent two-gap equations [29] for a clean superconductor in zero field to

calculate the components of the order parameters.

$$\Delta_n = \sum_{n'} \lambda_{nn'} \Delta_{n'} \int_0^{\omega_D} \frac{d\varepsilon}{\sqrt{\varepsilon^2 + \Delta_{n'}^2}} \tanh\left(\frac{\sqrt{\varepsilon^2 + \Delta_{n'}^2}}{2T}\right), \quad (2)$$

where Δ_n is the components, $\lambda_{nn'} = g_{nn'} N_{n'}$ (where $N_{n'}$ is the density of states in the n' gap) is the dimensionless coupling constant (between n and n' components), and ω_D is the Debye frequency.

$$\omega_D = T_c e^{-C} e^{1/\lambda} \pi/2, \quad (3)$$

where λ is the highest eigenvalue of the $\lambda_{nn'}$ matrix, T_c is the critical temperature, and C is the Euler constant. Here we only consider a two-gap model case, namely, two components, Δ_1 and Δ_2 for the larger and the smaller gap, respectively.

$$\Delta_1 = \sum_{n'=1}^2 \lambda_{1n'} \Delta_{n'} \int_0^{\omega_D} \frac{d\varepsilon}{\sqrt{\varepsilon^2 + \Delta_{n'}^2}} \tanh\left(\frac{\sqrt{\varepsilon^2 + \Delta_{n'}^2}}{2T}\right), \quad (4)$$

$$\Delta_2 = \sum_{n'=1}^2 \lambda_{2n'} \Delta_{n'} \int_0^{\omega_D} \frac{d\varepsilon}{\sqrt{\varepsilon^2 + \Delta_{n'}^2}} \tanh\left(\frac{\sqrt{\varepsilon^2 + \Delta_{n'}^2}}{2T}\right), \quad (5)$$

and $g_{11} = g_1$, $g_{12} = g_{21} = g_3$, and $g_{22} = g_2$, where g_1 and g_2 are the pair interaction constants of the first and second gaps, respectively. g_3 is the inter-band scattering between Copper pairs of the two gaps. For simplification, we considered that $\lambda_{12} = \lambda_{21}$.

We then applied the previously calculated gaps to the Ambegaokar-Baratoff [17] equation for the different tunneling channels [30, 31]

$$I_c R_n = \sum_i C_i \frac{\pi}{2} \frac{\Delta_i(T)}{e} \tanh\left(\frac{\Delta_i(T)}{2k_B T}\right), \quad (6)$$

where e is the elementary charge, k_B is the Boltzman constant, $\Delta_i(T)$ means the i gap of order parameters, and C_i is the ratio coefficient for the i channel (we note that $\sum_i C_i = 1$). The C_1 depends on the curvature near T_c of the I_c/I_{c0} experimental curve, which is generally narrow and corresponds to a smaller value than C_2, i.e., the probability of tunneling though the second channel is much higher than that of the first channel. Therefore, we must only consider the value of the second gap Δ_2 in the calculation of equations (4) and (5).

In MgB$_2$, the superconducting gap with lowest critical temperature contributes mainly to the tunneling current in a Josephson junction along the layers of the material. The reason for this is that the superconducting gap with a low critical temperature is formed on a 3D Fermi surface pocket, and the other gap is created on a 2D Fermi surface pocket along the layers, making it more difficult for the cooper pairs to tunnel [32, 33]. The simulation results for *s*-wave, *d*-wave, and two-gap models are given in figure 4. The data is obviously different from the single-gapped *s*-wave or *d*-wave, but suggest a multi-gap model. Considering the unequal T_c results for each gap, we obtained a relatively large value of λ_{12} (0.3587) and λ_{21} (0.1771). However, both of

should be ≪1 for the weak coupling case [34]. Consequently, the gaps should be strongly coupled. Thus, we fixed the T_c for both gaps as 35.1 K and obtained a fit result as shown in figure 4. Here, the corresponding parameters are as follows: $\lambda_{11} = 0.9610$, $\lambda_{12} = \lambda_{21} = 0.7543$, $\lambda_{22} = 0.3183$, $C_1 = 0.1069$, and $C_2 = 0.8931$. Note that C_2 is considerably larger than C_1, indicating that one gap dominates the Josephson tunneling.

Ota and co-workers [30, 31] calculated the *T*-dependence of $I_c R_n$ for a heterojunction between the Fe-based superconductors and a single-band BCS type superconductor (lead). They also indicated that the grain boundary junctions show similar behavior to that of the heterojunction. However, the $(I_c/I_{c0}) - (T/T_c)$ curve has different curvature near T_c from the experimental one in figure 4, mainly because we considered that all gaps participate in the tunneling in equal form. Additionally we compared the experimental data with calculations made for other types of order parameter symmetries that could be considered as candidates, standard single-gap *s*-wave and *d*-wave, for which we calculated and plotted the $(I_c/I_{c0}) - (T/T_c)$ curves (figure 4). Our results indicate that both single-gap models seem unlikely for the present experimental results, and instead, the two-gap model is a highly promising candidate. Nevertheless, we cannot fit the present experimental results by applying the two-gap model directly. This is because the microbridge consists of abundant grain boundary junctions, which are connected to each other via both parallel and series connections. We assume that the junctions are connected in series. Thus, a more accurate estimation should be as follows:

$$I_c R_n = \sum_j I_c^j R_n^j, \quad (7)$$

where, the normal resistances may vary in different junctions, resulting in differences in total normal resistance. However, the $(I_c/I_{c0}) - (T/T_c)$ curves of each junction should be synchronous due to the same superconducting gap. As a result, we can obtain the gap symmetry profile from the $(I_c/I_{c0}) - (T/T_c)$ calculation results, even though we can hardly estimate the magnitude of the gap function. Thus, the consistency between the two-gap model and the characteristics of the experimental $(I_c/I_{c0}) - (T/T_c)$ curve suggests the presence of two effective gaps with differential magnitude. The present result is in agreement with the presented belief from the scientific community that the family of iron-based superconductors is a multi-gap *s*-wave superconductor. Howeverm, our results are inconclusive in regards to the symmetry of the hidden gap, namely, whether it is $s_{\pm}$, s_{++} or even $s+id$-wave. Based on the ARPES and other measurements [35], the pairing symmetry was considered as pure *s*-wave for the BaK$_x$Fe$_2$As$_2$ with $x = 1$. For the optimal-doped Ba$_{1-x}$K$_x$Fe$_2$As$_2$ with $0.4 < x < 1$ however, the symmetry is still under active debate, although most results indicate that it should be a mixture state [8, 36], namely, the $s+is$-wave or $s+id$-wave.

4. Conclusions

In summary, the $Ba_{0.6}K_{0.4}Fe_2As_2$ microbridge with a width of about 20 μm consists of numerous grains connected with each other and forming grain boundaries. By tunneling current across grain boundaries, the IVCs of the microbridge showed the superconductor/normal-metal/superconductor-type Josephson tunnel junction characteristics. By applying microwave radiation with a frequency of 10 GHz, typical Shapiro steps were observed for the junctions. The temperature dependence of the critical current behaved as a pronounced kink at $T \sim 20$ K, which is clearly different from the result assuming the singlet symmetry of s- or d- wave. However, this is consistent with the presented model with two effective gaps of different magnitude and T_c. Our results support multi-gap symmetry as $s+is$ or $s+id$-wave.

References

[1] Kamihara Y, Watanabe T, Hirano M and Hosono H 2008 *J. Am. Chem. Soc.* **130** 3296
[2] Paglione J and Greene R L 2010 *Nat. Phys.* **6** 645
[3] Mazin I I 2010 *Nature* **464** 183
[4] Pillay D, Johannes M D and Mazin I I 2008 *Phys. Rev. Lett.* **101** 246808
[5] Kuroki K, Onari S, Arita R, Usui H, Tanaka Y, Kontani H and Aoki H 2008 *Phys. Rev. Lett.* **101** 087004
[6] Onari S and Kontani H 2009 *Phys. Rev. Lett.* **103** 177001
[7] Onari S, Kontani H and Sato M 2010 *Phys. Rev.* B **81** 060504
[8] Reid J P *et al* 2012 *Supercond. Sci. Technol.* **25** 084013
[9] Grafe H J *et al* 2008 *Phys. Rev. Lett.* **101** 047003
[10] Onari S, Kontani H and Sato M 2008 *J. Phys. Soc. Jpn.* **77** 023703
[11] Shimizu Y, Yamada T, Takami T, Niitaka S, Takagi H and Itoh M 2009 *J. Phys. Soc. Jpn.* **78** 123709
[12] Zhang X H, Oh Y S, Liu Y, Yan L Q, Kim K H, Greene R L and Takeuchi I 2009 *Phys. Rev. Lett.* **102** 147002
[13] Chen C T, Tsuei C C, Ketchen M B, Ren Z A and Zhao Z X 2010 *Nat. Phys.* **6** 260
[14] Richard P, Sato T, Nakayama K, Takahashi T and Ding H 2011 *Rep. Prog. Phys.* **74** 124512
[15] Gordon R T, Ni N, Martin C, Tanatar M A, Vannette M D, Kim H, Samolyuk G D, Schmalian J, Nandi S and Kreyssig A 2009 *Phys. Rev. Lett.* **102** 127004
[16] Li J *et al* 2012 *Phys. Rev.* B **85** 214509
[17] Hilgenkamp H and Mannhart J 2002 *Rev. Mod. Phys.* **74** 485
[18] Robertazzi R P, Kleinsasser A W, Laibowitz R B, Koch R H and Stawiasz K G 1992 *Phys. Rev.* B **46** 8456
[19] Stepantsov E, Tarasov M, Naito M, Tsukada A and Winkler D 2006 *Appl. Phys. Lett.* **89** 213111
[20] Iida K *et al* 2013 *Phys. Rev.* B **87** 104510
[21] Rall D, Il'in K, Iida K, Haindl S, Kurth F, Thersleff T, Schultz L, Holzapfel B and Siegel M 2011 *Phys. Rev.* B **83** 134514
[22] Katase T, Ishimaru Y, Tsukamoto A, Hiramatsu H, Kamiya T, Tanabe K and Hosono H 2011 *Nat. Commun.* **2** 409
[23] Hiramatsu H, Katase T, Kamiya T and Hosono H 2012 *J. Phys. Soc. Jpn.* **81** 011011
[24] Kidszun M, Haindl S, Thersleff T, Haenisch J, Kauffmann A, Iida K, Freudenberger J, Schultz L and Holzapfel B 2011 *Phys. Rev. Lett.* **106** 137001
[25] Gao Z, Togano K, Matsumoto A and Kumakura H 2014 *Sci. Rep.* **4** 4065
[26] Li J *et al* 2013 *Appl. Phys. Lett.* **103** 062603
[27] Durrell J H, Eom C B, Gurevich A, Hellstrom E E, Tarantini C, Yamamoto A and Larbalestier D C 2011 *Rep. Prog. Phys.* **74** 124511
[28] Seidel P 2011 *Supercond. Sci. Technol.* **24** 043001
[29] Zhitomirsky M E and Dao V H 2004 *Phys. Rev.* B **69** 054508
[30] Ota Y, Machida M, Koyama T and Matsumoto H 2010 *Phys. Rev.* B **81** 014502
[31] Ota Y, Nakai N, Nakamura H, Machida M, Inotani D, Ohashi Y, Koyama T and Matsumoto H 2010 *Phys. Rev.* B. **81** 214511
[32] Brinkman A, Golubov A A, Rogalla H, Dolgov O V, Kortus J, Kong Y, Jepsen O and Andersen O K 2002 *Phys. Rev.* B **65** 180517
[33] Ambegaokar V and Baratoff A 1963 *Phys. Rev. Lett.* **10** 486
[34] Zhitomirsky W E and Dao V H 2004 *Phys. Rev.* B **69** 054508
[35] Lin S Z, Maiti S and Chubukov A 2016 *Phys. Rev.* B **94** 064519
[36] Platt C, Thomale R, Honerkamp C, Zhang S C and Hanke H 2012 *Phys. Rev.* B **85** 180502(R)